RESEARCH ARTICLE

WILEY

Brain reserve affects the expression of cognitive reserve networks

Annabell Coors[1] | Seonjoo Lee[2,3] | Yunglin Gazes[1,4,5] | Margaret Gacheru[2,3] | Christian Habeck[1,4,5] | Yaakov Stern[1,4,5]

[1]Cognitive Neuroscience Division, Department of Neurology, Columbia University Vagelos College of Physicians and Surgeons, New York, New York, USA

[2]Mental Health Data Science, New York State Psychiatric Institute, New York, New York, USA

[3]Department of Psychiatry and Biostatistics, Columbia University, New York, New York, USA

[4]Taub Institute for Research in Alzheimer's Disease and the Aging Brain, Columbia University, New York, New York, USA

[5]Gertrude H. Sergievsky Center, Columbia University, New York, New York, USA

Correspondence
Yaakov Stern, Cognitive Neuroscience Division, Department of Neurology, Columbia University Vagelos College of Physicians and Surgeons, 630 W 168th St, P&S Box 16, New York, NY 10032, USA.
Email: ys11@cumc.columbia.edu

Funding information
Deutsche Forschungsgemeinschaft, Grant/Award Number: 519357857; National Institute on Aging, Grant/Award Numbers: R01AG026158, R01AG038465, R01AG062578

Abstract

Cognitive reserve (CR) explains differential susceptibility of cognitive performance to neuropathology. However, as brain pathologies progress, cognitive decline occurs even in individuals with initially high CR. The interplay between the structural brain health (= level of brain reserve) and CR-related brain networks therefore requires further research. Our sample included 142 individuals aged 60–70 years. National Adult Reading Test intelligence quotient (NART-IQ) was our CR proxy. On an in-scanner Letter Sternberg task, we used ordinal trend (OrT) analysis to extract a task-related brain activation pattern (OrT slope) for each participant that captures increased expression with task load (one, three, and six letters). We assessed whether OrT slope represents a neural mechanism underlying CR by associating it with task performance and NART-IQ. Additionally, we investigated how the following brain reserve measures affect the association between NART-IQ and OrT slope: mean cortical thickness, total gray matter volume, and brain volumes proximal to the areas contained in the OrT patterns. We found that higher OrT slope was associated with better task performance and higher NART-IQ. Further, the brain reserve measures were not directly associated with OrT slope, but they affected the relationship between NART-IQ and OrT slope: NART-IQ was associated with OrT slope only in individuals with high brain reserve. The degree of brain reserve has an impact on how (and perhaps whether) CR can be implemented in brain networks in older individuals.

KEYWORDS
capacity, interaction, Letter Sternberg task, neuropathology, ordinal trend analysis

Practitioner Points
- Older individuals with higher cognitive reserve (CR) showed a greater increase in brain network expression with higher cognitive load.
- The level of brain reserve impacts how (and perhaps whether) CR can be expressed in brain networks.

Annabell Coors and Seonjoo Lee contributed equally to the manuscript.

1 | INTRODUCTION

The concept of cognitive reserve (CR) refers to the adaptability of cognitive processes that helps to explain the differential susceptibility of cognitive abilities to brain aging, pathology, or insult (Stern et al., 2020). It has been observed that individuals with high CR can withstand more brain pathology before developing cognitive changes or dementia (Nelson et al., 2021). However, individuals with high CR have also been shown to have a more rapid cognitive decline and a shorter morbidity period once they become demented (Stern, 2012). The ability of a functional CR network to compensate likely depends on both the level of brain structure, which is referred to as brain reserve (Stern et al., 2020), and the level of CR. This suggests that age-related changes in brain structure can impact the functional networks that represent the neural implementation of CR. However, the bivariate relationship between the level of brain reserve and CR neural networks has not yet been investigated and is therefore the first research focus of this project. Second, we assessed the interaction between the level of CR and the level of brain reserve on the expression of CR neural networks. Both questions should contribute to a better mechanistic understanding of whether and how age-related brain changes impact the neural implementation of CR, that is, what link exists between brain reserve and CR.

Concerning the neural implementation of CR, it has been suggested that higher CR may be associated with neural networks that have greater efficiency or capacity, resulting in better performance in the presence of age- or disease-related brain changes (Stern, 2009). In previous studies, we have investigated the neural implementation of CR using the Letter Sternberg (LS) task (Habeck et al., 2022; Habeck, Rakitin, et al., 2005; Steffener et al., 2009; Stern et al., 2018; Zarahn et al., 2007). In this task (Sternberg, 1966), participants see one, three, or six letters. After a delay period, they are presented with a single letter and must indicate whether it was part of the studied set of letters. Because this task manipulates memory load via the variability in letter set size, individual differences in the increase in the pattern of task-related activation as load increases can provide information about the efficiency and capacity of network function. To optimally summarize changes in task-related activation across load, we used a multivariate technique called ordinal trend (OrT) analysis (Habeck, Krakauer, et al., 2005). This approach derives a single covariance pattern that summarizes task-related activation and whose expression increases with task load on an individual basis (Habeck et al., 2003, 2004, 2006; Habeck, Krakauer, et al., 2005; Habeck, Rakitin, et al., 2005). Thus, the OrT slope across the three-letter size conditions in the LS task can be used as an operationalization of network efficiency or capacity.

We have previously focused primarily on younger individuals and only calculated the OrT slope during the retention phase of the LS task (Habeck et al., 2022), so here we first wanted to test whether the OrT slope during the different LS task phases represents a measure of CR network expression in older individuals. To do this, we evaluated the associations of OrT slopes with the intelligence quotient (IQ) derived from the American National Adult Reading Test (NART-IQ), our proxy for CR, as well as with LS task performance. We

hypothesized (1) that CR is associated with increased expression of CR networks as measured by OrT slope and, through this association, with better LS task performance. We took NART-IQ as a proxy for CR, as this word reading test is assumed to reflect premorbid intelligence (Grober & Sliwinski, 1991) and has been repeatedly used as a proxy measure of CR, for example, by MacPherson et al. (2020).

We then investigated the impact of age-related morphometric measures that can reflect brain reserve (Stern et al., 2020), on the capacity of this putative CR network. We included mean cortical thickness, total gray matter volume, and brain volumes proximal to the areas contained in the OrT patterns (referred to as modulated volumes) as measures of brain reserve. Our focus was on older individuals, as they vary more in age-related morphometric measures than younger individuals. We tested the following hypothesis: (2) greater age-related declines in measures of brain morphometry, which indicates lower brain reserve, will be associated with reduced CR network expression (OrT slope).

Lastly, we evaluated whether brain reserve moderates the association between our CR proxy NART-IQ and level of CR network expression. We hypothesized that (3) our CR proxy interacts with brain reserve such that expression of CR-related brain networks depends on the level of brain reserve. Thus, this project goes a step further than previous publications by not only attempting to identify a measure of the neural implementation of CR, but also by examining CR neural network expression as a function of age-related differences in brain reserve. This provides new insights into how the concepts of brain reserve and CR are related.

2 | MATERIALS AND METHODS

2.1 | Participants

All participants were recruited for the Cognitive Reserve study (Stern, 2009) through random market mailing. Inclusion criteria were native English speakers, strongly right-handed, and at least a fourth-grade reading level. They were screened for magnetic resonance imaging (MRI) contraindications and hearing or visual impairment that would impede testing. Participants were free of medical or psychiatric conditions that could affect cognition. Careful screening ensured that the older participants did not meet criteria for dementia or mild cognitive impairment. For this study, we included 142 individuals aged 60–70 years.

2.2 | MRI acquisition

All magnetic resonance (MR) images were acquired in the same 3.0T Philips Achieva Magnet scanner with a standard quadrature head coil. All scans were acquired in one 2-h session. In addition to the functional magnetic resonance imaging (fMRI) sequences, all participants received magnetization-prepared rapid gradient echo (MPRAGE), arterial spin labeling (ASL), fluid-attenuated inversion recovery (FLAIR), and diffusion

tensor magnetic resonance imaging (DTI) scans. For the current study, only fMRI and MPRAGE sequence were considered. High-resolution T1-weighted MPRAGE scans were collected axially for each subject (repetition time (TR) = 6.6 ms, echo time (TE) = 3 ms, flip angle = 8°, field of view (FOV) = 256 × 256 mm, matrix size: 256 × 256 mm, slices: 165, voxel size = $1 \times 1 \times 1$ mm^3). fMRI data were acquired using T2*-weighted gradient-echo planar images sequence (TR = 2000 ms; TE = 20 ms; flip angle = 72°; FOV = 224 × 224 mm; voxel size = 2 mm × 2 mm; slice thickness = 3 mm; duration = 3.5 min). Task administration and data collection were controlled by a computer running E-Prime software, and electronically synchronized with the MR scanner. Task stimuli were back-projected onto a screen located at the foot of the MRI bed using an liquid-crystal display (LCD) projector. Subjects viewed the screen via a mirror system located in the head coil. Task responses were made on a LUMItouch response system and behavioral response data were recorded on the task computer. A neuroradiologist reviewed each participant's MRI scan and confirmed that there were no clinically significant findings for any of the participants.

2.3 | Cognitive examinations

Our implementation of the LS task (Sternberg, 1966) for fMRI consisted of a total of three runs of 30 trials each with three components per trial: stimulus, retention, and probe, followed by a 3 s inter-trial interval. The study component consisted of the simultaneous presentation of 3 s of either one, three, or six uppercase letters (10 of each trial type per run) arranged in a 2 × 3 grid. After a retention interval (7 s), a single lowercase letter was presented in the center of the screen for 3 s. During this period, participants were instructed to press one of two keys as quickly as possible, indicating whether this probe was part of the stimuli set. The contrasts selected in this study were the change in activation over the three set sizes (one, three, or six letters) separately for the stimulus, retention, and probe periods. Behavioral performance variables were recorded for each memory-load level as the reaction time for correct trials and the overall accuracy rate.

IQ was estimated with the American NART (Grober & Sliwinski, 1991; Nelson & O'Connell, 1978).

2.4 | Image analysis procedures

2.4.1 | fMRI pre-processing

We use FMRIB Software Library (FSL) v5.0 and custom-written Python code. The following steps were performed for each participant's data set: All functional images were realigned to the first volume, corrected for the order of slice acquisition, smoothed with a 5 mm^3 nonlinear kernel followed by intensity normalization, and high-pass filtered using a Gaussian kernel and cut-off frequency of 0.008 Hz. The first functional volume was co-registered to the

template-aligned T1-weighted image using FMRIB's Linear Image Registration Tool (FLIRT) with the normalized mutual information cost function. These obtained transformation parameters were used to transfer the statistical parametric maps of the subject-level analysis to standard space.

### 2.4.2 | fMRI subject-level time-series modeling

The fMRI time-series data were pre-whitened to explicitly correct for intrinsic autocorrelations in the data. The fMRI Expert Analysis Tool (FEAT) module in FSL was used for subject-level analysis. Event-related design was implemented with nine separate regressors for correct trials across memory loads (one, three, and six letters), with each load having three task phases (stimulus, retention, and probe). For all three loads, the stimulus phase lasts 3 s, retention 7 s, and probe lasts the duration of reaction time for the corresponding trial. The design matrix was convolved with a model of the hemodynamic response function, and the contrast images for each of the three phases across each of the three memory loads per participant were included in the OrT analysis described below.

2.4.3 | Ordinal trend analysis

OrT is a multivariate technique that can identify activation patterns for parametric designs that vary expression within subject by task difficulty (Habeck et al., 2003, 2004, 2006; Habeck, Krakauer, et al., 2005; Habeck, Rakitin, et al., 2005). The technique uses a special design matrix to boost variance contributions by such patterns that show within subject increases in pattern score with the task parameter of interest, in our case: memory load. The current version of the software used in this report incorporated the design matrix and fitting procedure of the aforementioned original papers, but slightly modified the test statistic to assume a simpler and more intuitive meaning than in the original version: the number of individuals violating the positive association of their pattern expression with memory load, operationalized as the number of people with negative slopes in their linear load relationship, that is,

$$\text{Pattern score}(\text{load}) = \text{load} \times \beta + \text{intercept} + \varepsilon, \text{where load} = \text{one,}$$
three, or six letters.

The number of people producing a negative slope, that is, $\beta < 0$, is now taken as the test statistic (=number of exceptions) to probe the significance of the load relationship of the derived activation pattern. A null distribution is readily generated by a permutation test of 1000 iterations for which load-assignments are randomized within the subject, and the whole analytic point-estimate derivation is repeated on the randomized data. The fraction of times the permutation test yields a number of exceptions as low or lower than the point estimate is taken as the p-value. For robustness of voxel loadings in the derived pattern, we used a simple bootstrap technique: the data were sampled
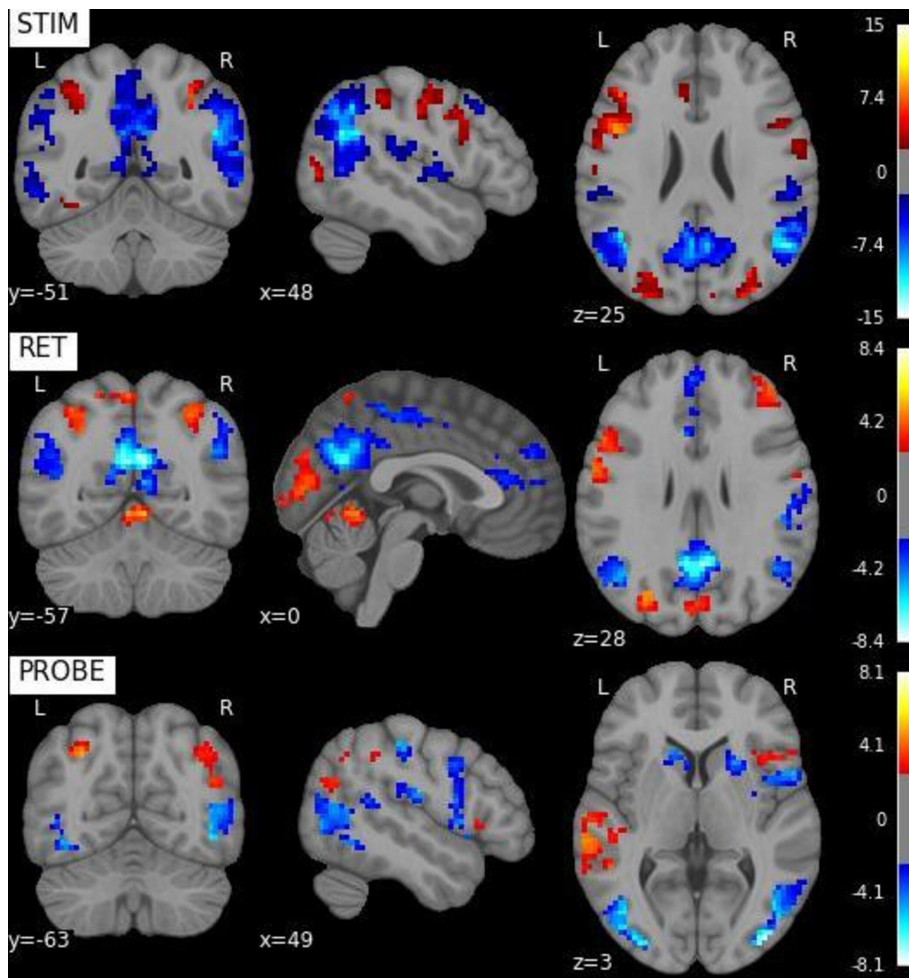
FIGURE 1 Covarying positive/negative brain networks. Task-positive brain networks are represented in red-yellow and the task-negative brain networks are represented in blue-cyan. The visualization is separately for the stimulus phase (STIM), retention phase (RET), and probe phase (PROBE) of the Letter Sternberg task.

with replacement without randomizing the subject and load-assignments, and the analytic point-estimate derivation was repeated 500 times from the resampled data. z-Values for the voxel loadings were computed as the ratio of the point estimate of the loading divided by the bootstrap standard deviation around this point estimate as:

$$z = \frac{\text{point estimate}}{\text{standard deviation}}.$$

The slopes of the OrTs were computed within subject by regressing pattern scores against the memory load levels (one, three, and six letters). The slopes were then converted to z-scores, and the task-positive and -negative networks were identified using the false discovery rate (FDR)-corrected thresholds for the three task phases (Figure 1 and Table 1).

2.4.4 | Computing modulated volume

We computed two variables for modulated volume. One for the volume of the gray matter proximal to the identified task positive networks and one for the volume of the gray matter proximal to the identified task-negative networks. To do so, we first constructed an optimal, population-specific template representing the average shape and intensity of the brain images of older participants utilizing a diffeomorphic shape and intensity averaging technique (Avants et al., 2008), as described in Kim et al. (2008). The custom template was derived from a set of randomly selected 30 individuals. The custom template procedure was fully automated following the antsMultivariateTemplateConstruction2.sh script. We used the region-based cross-correlation similarity metric. The maximum number of iterations in the normalization was set to 200, although convergence could occur before the maximum is reached. Normalization steps with the Advanced Normalization Tools (ANTs) included: (a) affine registration of the native-space gray matter images to a Montreal Neurological Institute (MNI) gray matter template (voxel size: $1 \times 1 \times 1$ mm^3); (b) creation of a template by averaging the affine-registered gray matter images; (c) nonlinear registration of the native-space gray matter images to the template; (d) creation of another template; (e) three extra iterations of the steps (c) and (d); and (f) nonlinear registration of the native-space gray matter images to the last template. Non-linear registrations were performed with the high-resolution diffeomorphic symmetric normalization (ANTs-SyN) (Avants et al., 2008). After computing the template, each native-space image was nonlinearly registered to the template, and the template to the $1 \times 1 \times 1$ mm^3 MNI template using ANTs, and the Jacobian of the deformation was computed for each image. Then, the modulated volumes were computed by multiplying the determinant of the Jacobian to each network mask.

TABLE 1 Brain regions included in the ordinal trend slopes.

Voxels in cluster	Max x	Max y	Max z	Brain regions
Stimulus positive				
32,859	−26	−7	−16	Left pre- and post-central gyri, putamen, caudate, inferior and middle frontal gyri
18,036	10	−34	−22	Bilateral thalami, right putamen, and brain stem
18,036	−35	−58	−16	Left lateral occipital cortex
11,016	46	−76	−4	Right lateral occipital cortex
10,962	10	−79	−7	Bilateral intracalcarine cortex and lingual gyrus
8586	−5	32	17	Bilateral paracingulate gyrus and anterior cingulate
8262	64	2	14	Right precentral gyri
Stimulus negative				
38,745	−2	−58	2	Bilateral precuneus, posterior cingulate, and cuneal cortex
34,317	61	−49	−10	Right angular gyrus, lateral occipital cortex, middle temporal gyrus, supramarginal gyrus, and opercular cortex
21,654	−59	−16	−19	Left lateral occipital cortex, angular gyrus, and middle temporal gyrus
8289	−38	−19	−7	Left central opercular cortex
4455	1	47	35	Left superior and middle frontal gyri
4428	40	14	35	Right middle frontal gyrus
Retention positive				
12,339	−56	5	−10	Left pre- and post-cental gyrus and inferior frontal gyrus
10,854	−32	−85	23	Left lateral occipital cortex and superior parietal lobule
10,179	−2	−58	−13	Cerebellum
5454	49	−28	38	Right superior parietal lobule and lateral occipital cortex
3618	40	41	11	Right frontal pole and middle frontal gyrus
2970	61	−7	26	Right pre- and post-central gyri
Retention negative				
12,825	10	−55	2	Bilateral precuneous and posterior cingulate
7533	10	−1	38	Bilateral precentral gyrus and supplementary motor cortex
7479	58	−4	−22	Right central opercular cortex and Heschl's gyrus
7128	−47	−73	5	Left occipital cortex and angular gyrus
4428	4	32	8	Bilateral anterior cingulate and paraculate gyri
3645	−38	−22	−4	Left Heschl's gyrus and central opercular cortex
3294	52	−61	23	Right lateral occipital cortex and angular gyrus
3078	64	−19	23	Right supramargial and post-central gyri
Probe positive				
14,094	−44	8	5	Left inferior and middle frontal gyri and precentral gyrus
8802	−5	35	17	Bilateral paracingulate and superior frontal gyrus
6453	−53	−22	−4	Left superior temporal and supramarginal gyri
4833	31	38	−19	Right insular and frontal orbital cortices
3456	52	−67	20	Right lateral occipital cortex and angular gyrus
3240	−35	−82	35	Left lateral occipital cortex and superior parietal lobule
Probe negative				
19,359	52	−52	−13	Right lateral occipital cortex and supramarginal gyrus
10,125	4	2	32	Bilateral supplementary motor cortex and anterior cingulate
8100	−41	−70	−13	Left lateral occipital cortex
6966	−29	2	−25	Left putamen and anterior cingulate
6183	58	8	−22	Right precentral gyrus and central opercular cortex

(Continues)

TABLE 1 (Continued)

Voxels in cluster	Max x	Max y	Max z	Brain regions
3834	34	−4	−25	Right putamen and amygdala
2862	−44	−34	38	Left post-central and supramarginal gyri

Note: The table lists those brain regions whose brain activation patterns are included in the ordinal trend slope. The ordinal trend slope was extracted separately for the three task phases (stimulus, retention, and probe) of the Letter Sternberg task. Regions listed are those that exceed 1500 voxels or top two regions. These brain regions are divided into positive and negative regions, with positive regions being those that showed higher activation with increasing task load and negative regions being those that were less activated with increasing task load.

The average volume values were computed for the positive/negative networks for each of the three task phases.

2.5 | Statistical analysis

Statistical analyses were performed using R (R Core Team, 2021). Each hypothesis was tested at the FDR-controlled significance level of $p_{FDR} < .05$. First, we tested the correlation between OrT slopes and task performance measures during the three phases (stimulus, retention, and probe) using Spearman's correlation. We considered accuracy and reaction time for each memory load (one, three, and six letters) as well as their slopes over the three loads as the performance measures. We additionally calculated the correlations between OrT slopes in the different task phases and NART-IQ. Second, we tested the associations of the structural brain reserve measures cortical thickness, gray matter volume, and modulated volumes of the OrT networks with OrT slopes using linear regression. Third, we correlated NART-IQ with the brain reserve measures controlling for estimated intracranial volume (eTIV) in the case of modulated volumes and gray matter volume. Moderation analysis assumes that a variable can only be a moderator if it is uncorrelated with the predictor (Kraemer et al., 2001). Since the brain reserve variables turned out to be uncorrelated with the predictor variable NART-IQ, we subsequently tested whether the relationships between NART-IQ and OrT slopes differ depending on the level of age-related brain pathology (i.e., brain reserve). We then explored the interactions in more detail using Johnson–Neyman plots, which visualize in which range of the moderator variable brain reserve the association between NART-IQ and OrT slope is significant. All regression models included age and sex as covariates. The models that included gray matter and modulated volumes were additionally adjusted for eTIV.

3 | RESULTS

3.1 | Demographic characteristics

Table 2 presents a summary of baseline demographics and OrTs slopes. In our sample, 55.6% were female. The participants had an average of about 16 years of education (minimum: 12 years, maximum: 22 years) and had an average NART-IQ of 118.24 (minimum: 94, maximum: 131). Reaction times showed a load-dependent increase (reaction time in the one-letter condition: M = 1.03 s,

TABLE 2 Baseline Characteristics of Participants.

| Age, years	Mean (SD)	64.96 (3.06)
Gender	F	79 (55.6%)
	M	63 (44.4%)
NART-IQ	Mean (SD)	118.24 (8.67)
Education, years	Mean (SD)	16.00 (2.35)
OrT stimulus slope	Mean (SD)	4.29 (1.84)
OrT retention slope	Mean (SD)	2.01 (0.76)
OrT probe slope	Mean (SD)	4.18 (2.47)

Abbreviations: NART-IQ, National Adult Reading Test intelligence quotient; OrT, ordinal trend; SD, standard deviation.

SD = 0.25 s; three-letter condition: M = 1.22 s, SD = 0.25 s, six-letter condition: M = 1.45 s, SD = 0.30 s). The mean accuracy was comparable in the one-letter and three-letter conditions, but mean accuracy was lower and varied more in the six-letter condition (one-letter condition: M = 96.6%, SD = 4.8%; three-letter condition: M = 96.1%, SD = 4.8%; six-letter condition: M = 91.2%, SD = 7.4%).

3.2 | Ordinal trend analysis

The OrT analysis successfully derived a common activation pattern for each of the three task phases, such that expression increased with task load for the corresponding task phase. For the stimulus phase, a pattern could be derived from principal components (PCs) 1–23 with three people violating the rule of positive memory slopes in their pattern expression (Figure 2). In the retention and probe phases, patterns were derived from PCs 1–48 and 1–46, respectively, with zero and seven people violating the rule of positive memory slopes (Figure 2). The relationships between task load and the derived patterns in all three task phases were significant at p < .001 as ascertained from a permutation test.

The average OrT slope was lower during the retention phase (mean = 2.01, SD = 0.76) in comparison to the OrT slopes during the stimulus (mean = 4.29, SD = 1.84) and probe (mean = 4.18, SD = 2.47) phases (Table 2). However, during the stimulus and probe phases, there were a few individuals who experienced a reduction in their OrT scores as the number of letters increased in the LS task (stimulus: minimum = −2.51; probe: minimum = −0.95). The covarying task-positive and -negative networks identified are visualized in Figure 1 and listed in Table 1. Across the three task phases, task-
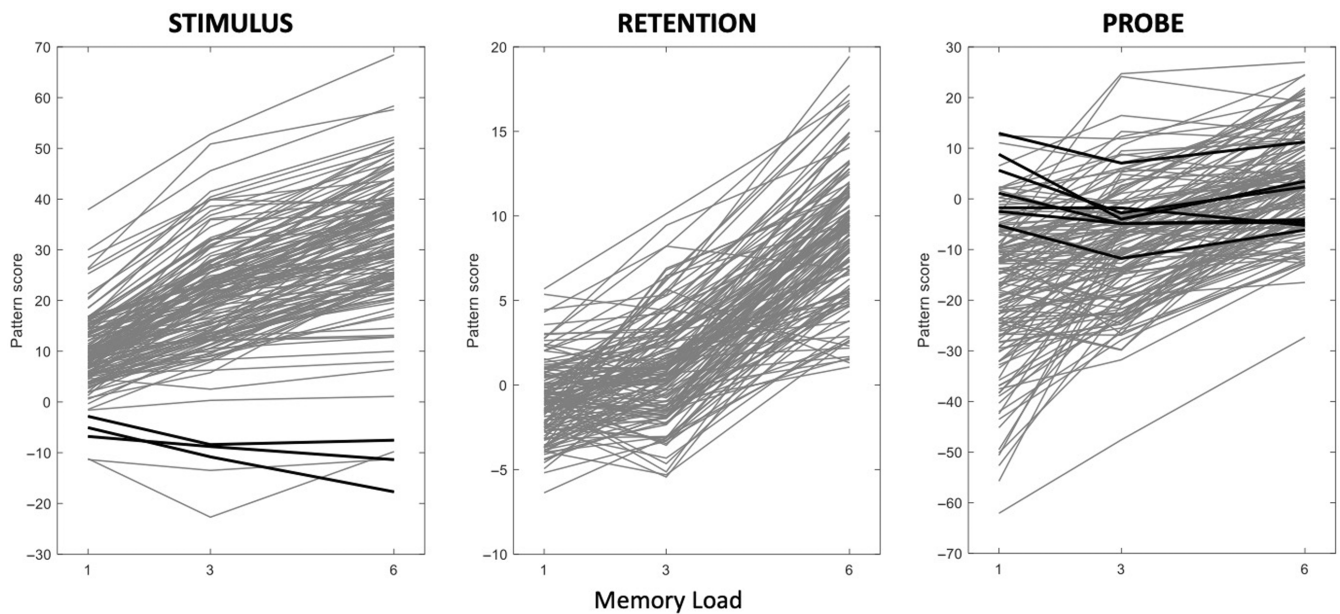
FIGURE 2 Task-related brain activation pattern curves. The curves are visualized separately for the three task phases of the Letter Sternberg (LS) task, starting on the left with the stimulus phase, then the retention phase, and the probe phase. For each phase, the memory load in the LS task is depicted on the *x*-axis (one, three, and six letters) and the brain activation pattern score is depicted on the *y*-axis. For the stimulus phase, a pattern could be derived from PCs 1–23 with three exceptions to the increasing pattern-slope rule. For the retention phase, a pattern was constructed from PCs 1–48 with zero exceptions. For the probe phase, a pattern was constructed from PCs 1–46 with seven exceptions.

positive regions included left inferior and middle frontal gyri, striatal areas, and bilateral occipital cortex. Task-negative regions included bilateral precuneus and superior parietal lobule.

3.3 | Relation of OrT slope to performance

We investigated the relationship between OrT slopes and indices of task performance during each of the three task phases. Overall, higher OrT slopes were associated with both more accurate and faster performance. The OrT slope during stimulus and probe correlated negatively with the average reaction time over the three set sizes and correlated positively with the average accuracy over the three set sizes (Table 3).

3.4 | Correlation of OrT slope with NART-IQ

The OrT slope during stimulus was positively correlated with NART-IQ (Spearman's correlation coefficient $r = 0.176$, $p = .038$). During probe phase this relationship was at the trend level ($r = 0.155$, $p = .069$). No correlation was found during retention ($r = -0.006$, $p = .946$).

3.5 | Relation of brain morphometry measures to OrT slope

The modulated volumes of positive and negative networks during the stimulus, retention, and probe phases were not associated with

the corresponding OrT slopes (p's >= .084) (Table S1). Mean cortical thickness was also not associated with the OrT slopes during the three different task phases (p's >= .095) (Table S1). Total gray matter volume was associated with the OrT slope during the probe phase before adjusting for multiple testing (p-value = .008) but not during the other two task phases (p's >= .120) (Table S1).

3.6 | Relation of brain morphometry measures to NART-IQ

Total gray matter volume and the modulated volumes of positive and negative networks during all three task phases showed small correlations with NART-IQ (Spearman $r = 0.3$ for all correlations), whereas mean cortical thickness was not significantly correlated with NART-IQ. However, since modulated volumes and total gray matter volume are confounded with eTIV, we calculated partial correlations controlling for this variable. We found that none of the volumetric outcomes were correlated with NART-IQ after controlling for eTIV (p-values >.109).

3.7 | The association between NART-IQ and OrT slope as a function of brain reserve

Modulated volumes in both positive and negative networks moderated the relationship between NART-IQ and OrT slopes during the stimulus phase. For the positive network: standardized $\beta = .278$, false discovery rate-controlled p-value (p_{FDR}) = .021. For the negative

network: standardized $\beta = .286$, $p_{FDR} = .021$ (see Table 4c,d). Total gray matter volume also moderated the association between NART-IQ and OrT slope (standardized $\beta = .250$, $p_{FDR} = .048$) in the stimulus phase but mean cortical thickness did not (see Table 4a,b). None of the structural brain reserve measures moderated the associations between NART-IQ and OrT slopes in the retention and probe phase (Tables S2 and S3).

As seen in the Johnson–Neyman plot in Figure 3, during the stimulus phase the association between IQ and OrT slope was significant in people with higher values in the structural brain reserve measures. In Figure 3, the x-axis represents the four different structural measures of brain reserve. The y-axis represents the degree to which NART-IQ as a proxy for CR is related to CR network expression (OrT slope). More positive values on the y-axis indicate a stronger relationship between CR and expression of the CR-related networks. Note that for all three plots it holds true that with increasing brain reserve, the relationship between CR and the level of expression of the CR-related networks gets stronger. Note also, that below brain reserve values of $z \sim 0$, there is no longer any link between CR and the level of expression of CR-related networks. CR relates to the level of CR network expression at very low levels of brain reserve in the case of the modulated volumes and gray matter volume, but the y-axis shows that this effect is negative: higher CR is associated with lower expression of CR-related networks in individuals with low brain reserve. However, there were only three individuals with volumetric measures below a z-value of -2. Therefore, the association between NART-IQ and OrT slope in the very low brain reserve range is an estimate by the model that might not be very reliable.

TABLE 3 Correlation between ordinal trend (OrT) slopes and task performance measures.

CR network function (OrT slope)	Performance measures	Spearman's correlation coefficient	p-Value
Stimulus	Accuracy slope	−0.009	.920
	Average accuracy	0.228[*,a]	.007
	RT slope	0.093	.277
	Average RT	−0.220[*,a]	.009
Retention	Accuracy slope	−0.030	.724
	Average accuracy	0.159	.061
	RT slope	0.051	.548
	Average RT	0.065	.445
Probe	Accuracy slope	−0.093	.275
	Average accuracy	0.296[**,a]	<.001
	RT slope	0.232[*]	.006
	Average RT	−0.388[***,a]	<.001

Abbreviation: p_{FDR}, false discovery rate-controlled significance level; RT, reaction time.

[a]False discovery rate-controlled p-value <.05.

[*]$p_{FDR} < .05$; [**]$p_{FDR} < .01$; [***]$p_{FDR} < .001$.

TABLE 4 Regression results to test the effects of structural brain reserve measures (mean thickness, total gray matter volume, and modulated volumes for positive and negative networks) and National Adult Reading Test intelligence quotient (NART-IQ) moderation on slopes of the ordinal trend (OrT) networks during the stimulus phase.

Predictors	(a) Mean thickness			(b) Total gray matter volume		
	Std. β	Std. CI	p	Std. β	Std. CI	p
Brain measure	−.006	−0.182 to 0.169	.944	.078	−0.262 to 0.418	.649
NART-IQ	.221	0.046 to 0.396	.014	.215	0.032 to 0.397	.021
Intracranial volume				.015	−0.312 to 0.343	.925
Sex (M)	−.044	−0.388 to 0.300	.802	−.153	−0.588 to 0.281	.486
Age	.079	−0.098 to 0.256	.377	.092	−0.093 to 0.277	.326
Brain measure × NART-IQ	.147	−0.025 to 0.318	.092	**.250[a]**	**0.056 to 0.444**	**.012[*,a]**

Predictors	(c) Positive network			(d) Negative network		
	Std. β	Std. CI	p	Std. β	Std. CI	p
Modulated volume	−.378	−0.757 to −0.000	.050	−.120	−0.506 to 0.265	.538
NART-IQ	.236	0.061 to 0.410	.008	.215	0.039 to 0.392	.017
Intracranial volume	.406	0.012 to 0.799	.043	.178	−0.219 to 0.574	.377
Sex (M)	−.080	−0.499 to 0.339	.707	−.148	−0.573 to 0.276	.490
Age	.038	−0.127 to 0.203	.649	.058	−0.108 to 0.225	.490
Modulated volume × NART-IQ	**.278[a]**	**0.096 to 0.460**	**.003[*,a]**	**.286[a]**	**0.096 to 0.476**	**.004[*,a]**

Note: All regression models included age and sex as covariates. The models that included gray matter and modulated volumes were additionally adjusted for total intracranial volume.

Abbreviations: CI, confidence interval; Std., standardized. Bold values are considered statistically significant.

[a]False discovery rate-controlled p-value <.05.

[*]$p_{FDR} < .05$
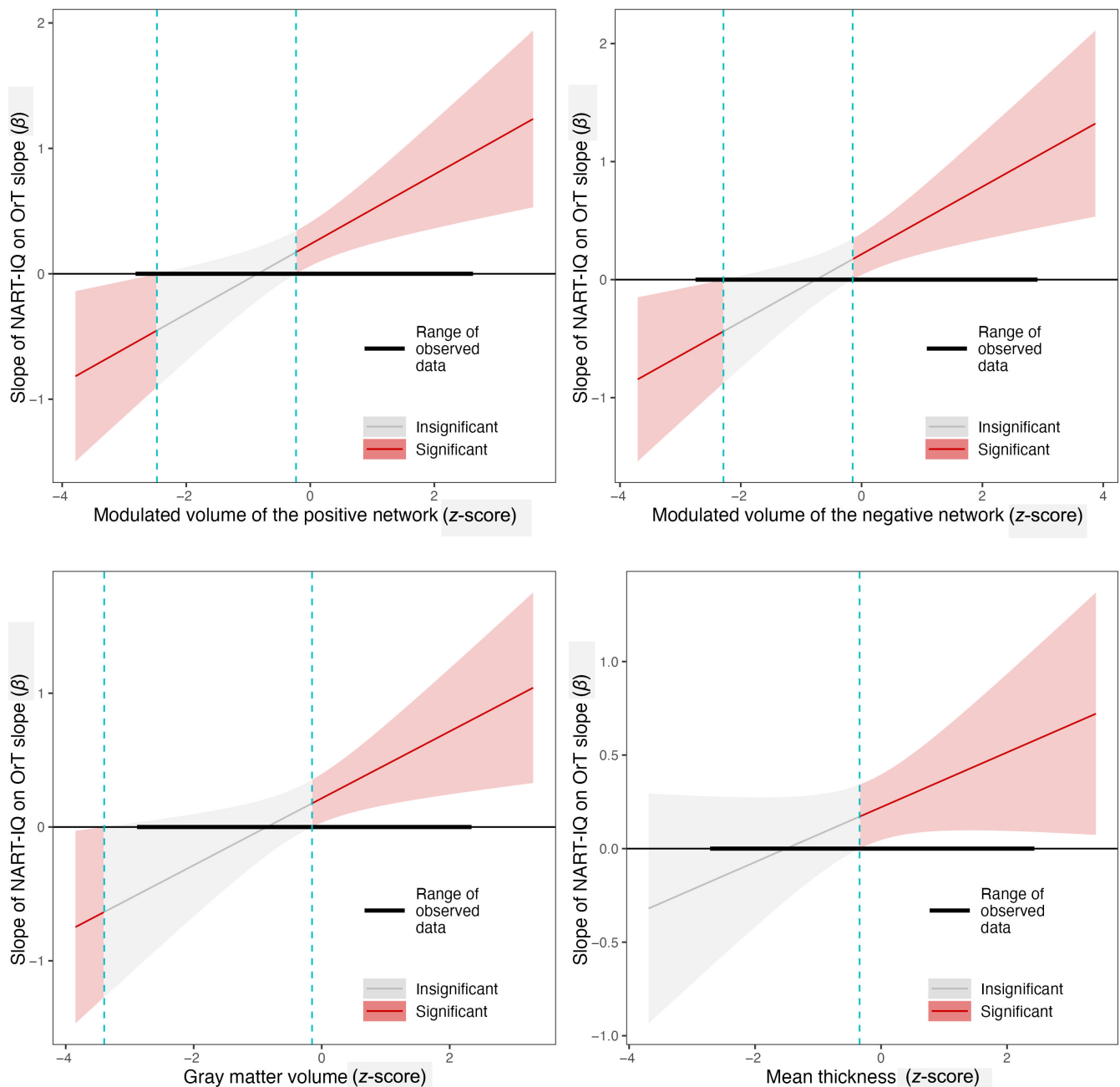
FIGURE 3 Johnson–Neyman plot for the effect of brain reserve (mean thickness, total gray matter volume, and modulated volumes of the positive and negative networks) moderation with National Adult Reading Test intelligence quotient (NART-IQ) on ordinal trend (OrT) slopes during the stimulus phase. The *x*-axis of each plot represents one of the four structural brain reserve measures. The *y*-axis represents the degree to which NART-IQ as a proxy for cognitive reserve (CR) impacts CR network expression (OrT slope). Positive values on the *y*-axis mean that the association between CR and CR network expression becomes stronger with higher levels of CR. We colored the range of CR values for which the moderation effect is significant in red and the other part in grey. The area around the regression lines indicates the 95% confidence interval.

4 | DISCUSSION

We investigated whether the OrT slope during the different phases of the LS task represents a neural implementation of CR in 142 on average highly educated participants above the age of 60 years. We then asked whether brain reserve impacts this neural implementation of CR.

Higher OrT slope was associated with better performance, that is, higher accuracy and faster reaction time, during the stimulus and probe phases. Further, the OrT slope during the stimulus phase was positively correlated with NART-IQ. This was also seen at trend level during the probe phase. Thus, the steeper the increase in the activation of the load-dependent network across the three task conditions, the better the performance and the higher the CR. These results stand

in contrast to the findings from our early study of young adults in which we also used the LS task and found that a *lower* OrT slope was associated with better performance and higher CR (Habeck, Rakitin, et al., 2005). These contrasting patterns likely result from the different mean age in our samples. In our previous study, the participants were in their twenties, whereas in this study our participants were above the age of 60 years. This explanation is supported by our recent study in which we directly compared young and old participants and found opposite patterns between OrT slope and task accuracy in the LS task (Habeck et al., 2022). However, in that study we had focused only on OrT slopes and task performance during the retention phase, as the associations in younger participants were mainly observed in the retention phase (Habeck et al., 2022). In this analysis, we took all three task phases into account and observed associations with CR in the stimulus and probe phases. The average OrT slope and its standard deviation were lower during the retention phase compared to the stimulus and probe phases. As a lower variation in the predictor variable leads to a smaller effect size, the statistical power to detect associations with the OrT slope was likely reduced in the retention phase.

A lower mean OrT slope during the retention phase might indicate that the brain activation level was on average very high in all set size conditions of the retention phase. Since we have previously demonstrated that LS task-related network activation increases with age (Zarahn et al., 2007), we strongly assume that the older individuals activated their brain networks in all task phases more than the younger ones. Therefore, their scope to increase brain activation with increasing task difficulty was limited and eventually reached a capacity limit. If they reached a capacity limit, one would expect this to result in poorer cognitive performance. And indeed, our current older sample had slightly higher reaction times on average than the younger sample and showed a drop in recognition accuracy in the six-letter task condition compared to the other two set size conditions. In the younger sample, accuracy did not decrease in the six-letter task condition (Habeck, Rakitin, et al., 2005). Thus, our findings indicate that those older individuals who could increase their activation levels the most across all three set size conditions are the ones with the highest capacity. The drop in accuracy also indicates that task demands were on average high for our older participants. In addition, the variation in CR level and thus OrT slope was generally limited as the NART-IQ ranged from 94 to 131, suggesting that there were no individuals with very low CR in our sample. This may have also reduced our statistical power to detect associations in other task phases.

Concerning the associations between OrT slopes with LS task performance and NART-IQ that we found in the stimulus and probe phase, it is possible that we have found associations in this sample but not in younger participants due to the strong visual component of these task phases (Habeck, Rakitin, et al., 2005). Interindividual variability in the activation of the visual areas is likely larger in older individuals compared to younger ones since sensory processing becomes more difficult in older age (Cabeza et al., 2004). The relevance of visual processing for successful task performance in older individuals is further supported by the inclusion of the bilateral occipital cortex as

task-positive network into the load-dependent brain activation pattern (Joukal, 2017).

The brain morphometry measures mean cortical thickness, total gray matter volume, and modulated volumes of the OrT networks that represent measures of brain reserve were not directly associated with network capacity/the level of expression of CR-related networks. However, we found that those measures affected the relationship between CR and level of CR network expression in the stimulus phase. When we used the Johnson–Neyman technique to investigate these interactions in more detail, we found that CR was only related to the level of CR network expression when brain reserve was high (z-score $\sim$ >0). This fits with the finding that brain reserve and CR are two independent constructs but suggests that the level of brain reserve affects how CR can be implemented. Its exact role, for example, if low brain reserve prevents an efficient implementation of CR or leads to a different neural implementation, requires future research. Given that the age range in our sample was 60–70 years, it can be assumed that enough variation in age-related brain pathologies was present, which might not be the case in a younger sample. However, the range of CR level was limited as our sample included on average highly educated individuals.

Future studies should assess whether a low task difficulty level would reverse the association between OrT slope and task performance and NART-IQ in older individuals, so that then, as in young individuals, lower OrT slope is associated with better performance and higher NART-IQ. Further, the interactions between brain reserve, CR, and CR brain network expression should also be investigated in a younger sample to test whether our findings are generalizable to the whole adult lifespan despite a potentially smaller variation in age-related brain pathologies.

5 | CONCLUSION

Overall, our findings elucidate the complex interactions between brain reserve measures, CR network expression, and CR that can underlie cognitive performance. We conclude that the level of brain reserve affects how (and perhaps whether) CR can be implemented in the brain.

CONFLICT OF INTEREST STATEMENT
The authors have declared no conflicts of interest for this manuscript.

DATA AVAILABILITY STATEMENT

The data that support the findings of this study are available from the corresponding author upon reasonable request.

ORCID

Annabell Coors https://orcid.org/0000-0001-9000-6390
Christian Habeck https://orcid.org/0000-0001-9961-7446

REFERENCES

Avants, B. B., Epstein, C. L., Grossman, M., & Gee, J. C. (2008). Symmetric diffeomorphic image registration with cross-correlation: Evaluating automated labeling of elderly and neurodegenerative brain. *Medical Image Analysis*, 12, 26–41.

Cabeza, R., Daselaar, S. M., Dolcos, F., Prince, S. E., Budde, M., & Nyberg, L. (2004). Task-independent and task-specific age effects on brain activity during working memory, visual attention and episodic retrieval. *Cerebral Cortex*, 14, 364–375.

Grober, E., & Sliwinski, M. (1991). Development and validation of a model for estimating premorbid verbal intelligence in the elderly. *Journal of Clinical and Experimental Neuropsychology*, 13, 933–949.

Habeck, C., Gazes, Y., & Stern, Y. (2022). Age-specific activation patterns and inter-subject similarity during verbal working memory maintenance and cognitive reserve. *Frontiers in Psychology*, 13, 852995.

Habeck, C., Hilton, H. J., Zarahn, E., Brown, T., & Stern, Y. (2006). An event-related fMRI study of the neural networks underlying repetition suppression and reaction time priming in implicit visual memory. *Brain Research*, 1075, 133–141.

Habeck, C., Hilton, H. J., Zarahn, E., Flynn, J., Moeller, J., & Stern, Y. (2003). Relation of cognitive reserve and task performance to expression of regional covariance networks in an event-related fMRI study of nonverbal memory. *NeuroImage*, 20, 1723–1733.

Habeck, C., Krakauer, J. W., Ghez, C., Sackeim, H. A., Eidelberg, D., Stern, Y., & Moeller, J. R. (2005). A new approach to spatial covariance modeling of functional brain imaging data: Ordinal trend analysis. *Neural Computation*, 17, 1602–1645.

Habeck, C., Rakitin, B. C., Moeller, J., Scarmeas, N., Zarahn, E., Brown, T., & Stern, Y. (2004). An event-related fMRI study of the neurobehavioral impact of sleep deprivation on performance of a delayed-match-to-sample task. *Cognitive Brain Research*, 18, 306–321.

Habeck, C., Rakitin, B. C., Moeller, J., Scarmeas, N., Zarahn, E., Brown, T., & Stern, Y. (2005). An event-related fMRI study of the neural networks underlying the encoding, maintenance, and retrieval phase in a delayed-match-to-sample task. *Cognitive Brain Research*, 23, 207–220.

Joukal, M. (2017). Anatomy of the human visual pathway. In K. Skorkovská (Ed.), *Homonymous visual field defects* (pp. 1–16). Springer International Publishing AG.

Kim, J., Avants, B., Patel, S., Whyte, J., Coslett, B. H., Pluta, J., Detre, J. A., & Gee, J. C. (2008). Structural consequences of diffuse traumatic brain injury: A large deformation tensor-based morphometry study. *NeuroImage*, 39, 1014–1026.

Kraemer, H. C., Stice, E., Kazdin, A., Offord, D., & Kupfer, D. (2001). How do risk factors work together? Mediators, moderators, and independent, overlapping, and proxy risk factors. *The American Journal of Psychiatry*, 158, 848–856.

MacPherson, S. E., Allerhand, M., Gharooni, S., Smirni, D., Shallice, T., Chan, E., & Cipolotti, L. (2020). Cognitive reserve proxies do not differentially account for cognitive performance in patients with focal frontal and non-frontal lesions. *Journal of the International Neuropsychological Society*, 26, 739–748.

Nelson, H. E., & O'Connell, A. (1978). Dementia: The estimation of premorbid intelligence levels using the New Adult Reading Test. *Cortex*, 14, 234–244.

Nelson, M. E., Jester, D. J., Petkus, A. J., & Andel, R. (2021). Cognitive reserve, Alzheimer's neuropathology, and risk of dementia: A systematic review and meta-analysis. *Neuropsychology Review*, 31, 233–250.

R Core Team. (2021). *R: A language and environment for statistical computing*. R Foundation for Statistical Computing.

Steffener, J., Brickman, A. M., Rakitin, B. C., Gazes, Y., & Stern, Y. (2009). The impact of age-related changes on working memory functional activity. *Brain Imaging and Behavior*, 3, 142–153.

Stern, Y. (2009). Cognitive reserve. *Neuropsychologica*, 47, 2015–2028.

Stern, Y. (2012). Cognitive reserve in ageing and Alzheimer's disease. *Lancet Neurology*, 11, 1006–1012.

Stern, Y., Arenaza-Urquijo, E. M., Bartrés-Faz, D., Belleville, S., Cantilon, M., Chetelat, G., Ewers, M., Franzmeier, N., Kempermann, G., Kremen, W. S., Okonkwo, O., Scarmeas, N., Soldan, A., Udeh-Momoh, C., Valenzuela, M., Vemuri, P., & Vuoksimaa, E. (2020). Whitepaper: Defining and investigating cognitive reserve, brain reserve, and brain maintenance. *Alzheimer's & Dementia*, 16, 1305–1311.

Stern, Y., Gazes, Y., Razlighi, Q., Steffener, J., & Habeck, C. (2018). A task-invariant cognitive reserve network. *NeuroImage*, 178, 36–45.

Sternberg, S. (1966). High-speed scanning in human memory. *Science*, 153, 652–654.

Zarahn, E., Rakitin, B., Abela, D., Flynn, J., & Stern, Y. (2007). Age-related changes in brain activation during a delayed item recognition task. *Neurobiology of Aging*, 28, 784–798.

SUPPORTING INFORMATION

Additional supporting information can be found online in the Supporting Information section at the end of this article.